



LAWRENCE
LIVERMORE
NATIONAL
LABORATORY

UCRL-PROC-234411

Simulations of high-mode Rayleigh-Taylor growth in NIF ignition capsules

B. A. Hammel, M. J. Edwards, S. W. Haan, M. M.
Marinak, M. Patel, H. Robey, J. Salmonson

September 7, 2007

5th International Conference on Inertial Fusion Sciences and
Applications

Kobe, Japan

September 9, 2007 through September 14, 2007

Disclaimer

This document was prepared as an account of work sponsored by an agency of the United States government. Neither the United States government nor Lawrence Livermore National Security, LLC, nor any of their employees makes any warranty, expressed or implied, or assumes any legal liability or responsibility for the accuracy, completeness, or usefulness of any information, apparatus, product, or process disclosed, or represents that its use would not infringe privately owned rights. Reference herein to any specific commercial product, process, or service by trade name, trademark, manufacturer, or otherwise does not necessarily constitute or imply its endorsement, recommendation, or favoring by the United States government or Lawrence Livermore National Security, LLC. The views and opinions of authors expressed herein do not necessarily state or reflect those of the United States government or Lawrence Livermore National Security, LLC, and shall not be used for advertising or product endorsement purposes.

Simulations of high-mode Rayleigh-Taylor growth in NIF ignition capsules

B.A. Hammel, M. J. Edwards, S.W. Haan, M.M. Marinak, M. Patel, H. Robey and
J. Salmonson

Lawrence Livermore National Laboratory

Livermore CA, U.S.A.

Email: hammel1@llnl.gov

Abstract

Near the pusher/fuel interface in the NIF indirect drive ignition capsule, the cold dense fuel can reach higher density than the material accelerating it. Unlike the outer surface where ablative stabilization is important, Rayleigh-Taylor (R-T) growth at this interface is stabilized only by the density gradient, plasma viscosity and mass diffusion. Simulations in HYDRA, with only gradient stabilization, indicate for the “Rev 1” design¹ a final mix width $> 30 \mu\text{m}$, resulting in $>10\%$ Be in the outer $\sim 25\%$ of the DT fuel. No degradation in the capsule neutron yield is observed. The R-T growth can be reduced by increasing the Cu fraction in the Be ablator, thereby increasing the Be density near the interface. To optimize designs, we are performing highly resolved 2D and 3D HYDRA simulations of capsules seeded with a surface spectrum up to modes ~ 2000 .

Introduction

In the indirect drive NIF target, the innermost region of the Be ablator is shielded from the drive x-rays by outer layers of Be that are doped with varying amounts of Cu.¹ The shielding reduces the heating of the innermost layer, keeping the density high so as to accelerate the dense DT with minimum instability growth. A profile of the density and temperature, for a “Rev 1” target as the capsule approaches peak velocity, is shown in Fig. 1. The difference in the heating of the Be and the relatively transparent DT is apparent in the rapid rise in the temperature across the interface. The DT fuel closest to the interface is heated by the hotter Be through thermal conduction, causing its density to drop. Similarly, the Be closest to the interface is cooled, and its density increases.

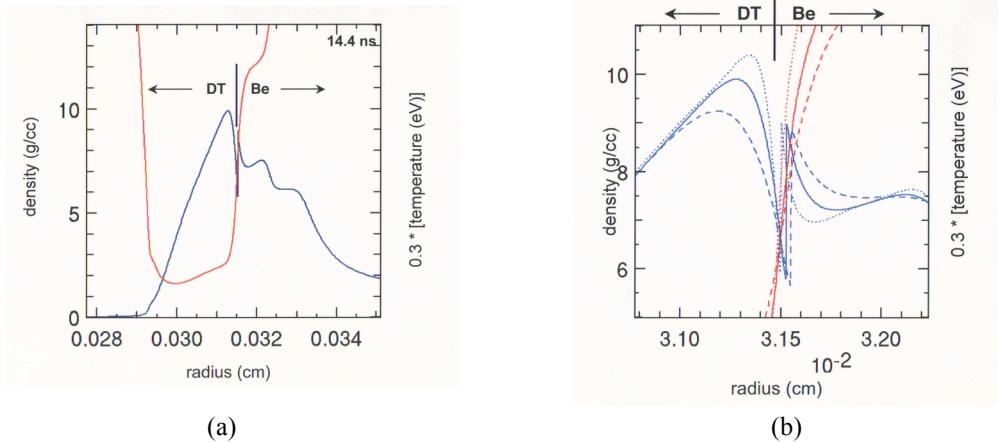


Figure 1. a) Radial profile, from a HYDRA² simulation during the implosion (14.4 ns), of the capsule density (g/cc) [blue] and $0.3 \times$ temperature (eV) [red]; b) Variation in the profiles for 0.3, 1.0, and 3.0 times the nominal thermal conductivity (Lee-More).

At an imbedded interface, without ablative stabilization, and neglecting viscosity and mass diffusion, the R-T growth rate is given by $\gamma_{RT} = \sqrt{Ak g / (1 + Ak L_\rho)}$ where the mode number $k = 2\pi/\lambda$, the Atwood number $A = (\rho_2 - \rho_1)/(\rho_2 + \rho_1)$, and g is the acceleration. The growth rate increases for shorter wavelengths until the wavelength is small compared to the density gradient scale length, $kL_\rho \gg 1$, where it is then limited to $\gamma_{RT} = \sqrt{g/L_\rho}$. For an initial perturbation at the interface describe by a power spectrum that decreases in amplitude with increasing k , the dominant mode after growth will be at a wavelength comparable to the scale length. The gradient scale length for the DT and Be in the region of their interface is determined by the thermal conductivity in the two materials. For the density profile at the time shown in Fig. 1, $L_\rho \approx 2 \mu\text{m}$.³ It is important to note, however, that thermal conductivity models are uncertain in this regime ($\sim 10 \text{ g/cc}$, $\sim 30 \text{ eV}$), and not confirmed by experiment. The effect on the density profile from multiplying the Lee-More⁴ conductivity by an arbitrary factor of 0.3 and 3.0 is shown in Fig. 1b. In 2D simulations with a perturbation at the interface, we observe a corresponding change in growth rate and final mix thickness. For the studies described below, we generally use Purgatorio conductivities.⁵

Results

All simulations reported here are performed with HYDRA.² To resolve the R-T growth for modes $m = 2\pi r/\lambda \approx 1000\text{-}2000$ requires $\sim 60\text{-}110$ angular zones/deg, and ~ 1000 radial zones distributed so that a resolution of $\leq 0.1 \mu\text{m}/\text{zone}$ is attained at the ablation front, the DT interface, and the inner DT surface. The roughness at the surfaces of the Be capsule are specified by either a random sum of modes with amplitudes determined by a power spectrum (PS),⁶ or an actual measured surface. For the latter case, we use data from a spherical interferometer (SI) developed in collaboration with General Atomics.⁷

Results from a simulation of an 18° wedge on the equator, with PS roughness on both the inner and outer surfaces of the Rev 1 (300 eV peak drive temperature) Be capsule is show in Fig. 2.

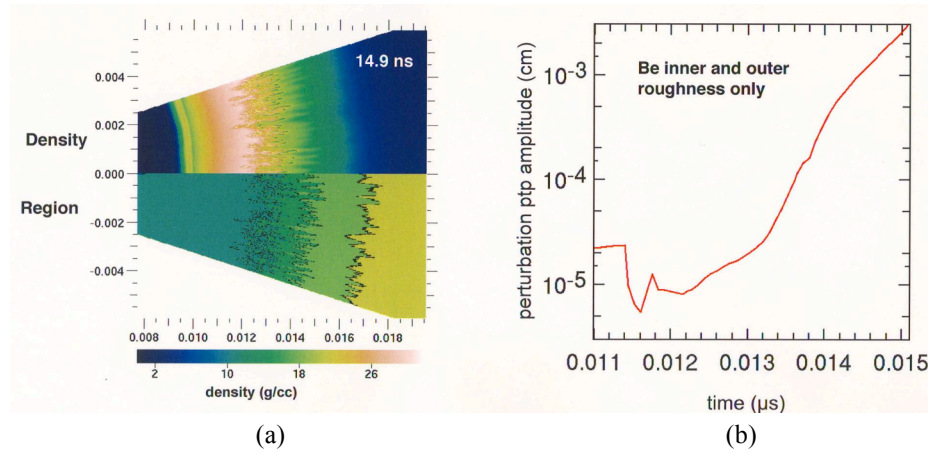


Figure 2. (a) Density and Material Region (Left to right: DT, Be, Be+0.35% Cu, Be+0.7% Cu) at 14.9 ns. (b) Perturbation peak-to-peak amplitude vs. time.

Fig. 2a shows a pseudo color plot of the density in the upper half of the picture and a material region plot in the lower half, both at 14.9 ns when the capsule has reached peak implosion velocity. Short wavelength (mode ~ 1000) perturbations are apparent at the interface between the DT and Be. The time dependent mix width at the DT:Be interface, plotted in Fig 2b, grows to $\sim 30 \mu\text{m}$.⁸ A reduction in growth rate is apparent after ~ 14 ns once the perturbation amplitude is comparable to the wavelength, consistent with the onset of saturation. The mass fraction of Be at a given radius vs. fractional DT fuel mass inside that radius is shown in Fig. 3. For this case, the outer 30% of the fuel contains more than 10% Be by mass. This capsule ignited and burned in the simulation, producing over 11 MJ. The mix fraction from a simulation with a smooth Be capsule, and with roughness only on the inner DT ice surface is also shown.⁹ In this case the perturbation grows after it is seeded at the interface by the shock reflected from the rough ice surface.

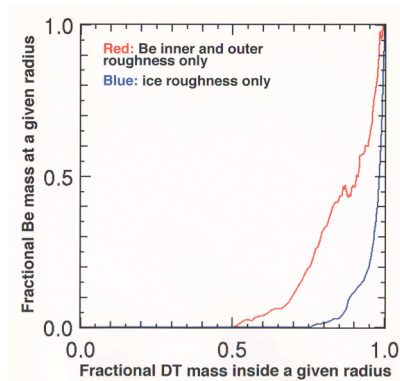


Figure 3. The mass fraction of Be at a given radius vs. fractional DT fuel mass inside that radius, when the core temperature is 8 keV (15.2 ns). Roughness on the inner and outer Be shell only [Red]. Roughness on the DT ice surface only [Blue].

Actual measured surfaces of Be capsules from the SI contain small, localized “defects”. Results from a 3D HYDRA simulation ($4.5^\circ \times 4.5^\circ$ equatorial segment) using measured roughness for the inner and outer Be surface are shown in Fig. 4. For this simulation, the inner surface was chosen to include a region with several > 20 nm defects to assess their effect on the mix region. For this case, the simulated mix width grows to $50 \mu\text{m}$ by peak velocity. The mass fraction of mixed Be is shown in Fig 4b. The simulation indicates that fingers of Be will penetrate through 75% of the fuel. Note however, that the mass fraction corresponding to these fingers is dependent on the number of defects in the simulated region. From the interferometer record studied for this simulation, defects greater than 20 nm are $\sim 10 \times$ more numerous per unit solid angle in the small patch used in the simulation than in the full data record. This implies a $\sim 10 \times$ reduction in total mass fraction at a given radius for the deeply penetrated material.

In the Rev 2 design (285 eV peak drive temperature),¹⁰ a higher Cu fraction is used in the doped Be layers to mitigate high mode growth by decreasing the heating of the innermost Be layer, and increasing its density in the region of the interface. This significantly improves the stability of high modes as seen in Fig. 5, where we compare 2D simulations of both Rev 2 and Rev 1 designs with the roughness of the inner Be surface taken from a “line-out” through the measured 3D roughness so as to include several > 20 nm defects. This Rev 1 2D “line-out” simulation is also compared to the 3D simulation in Fig. 4b.

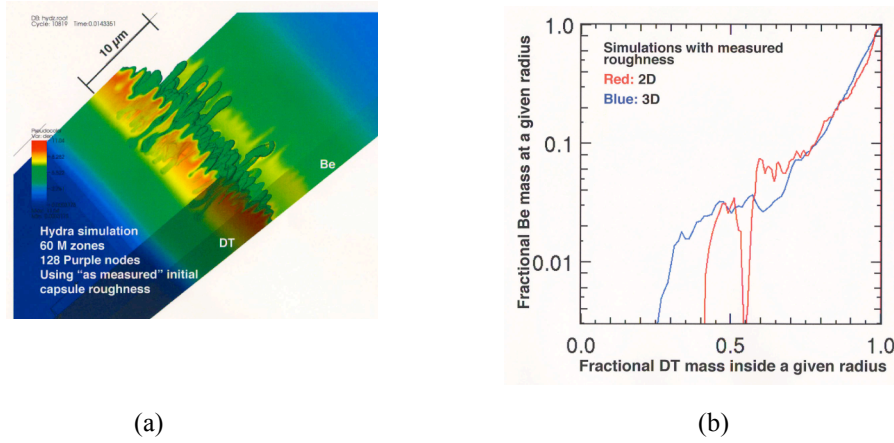


Figure 4. (a) Pseudo color plot of density at 14.3 ns from a 3D simulation of Rev 1 target with measured roughness on inner and outer Be surfaces. (b) Mass fraction of Be vs. fractional fuel mass for 3D (blue) and 2D (red) simulations, when the core temperature is 8 keV.

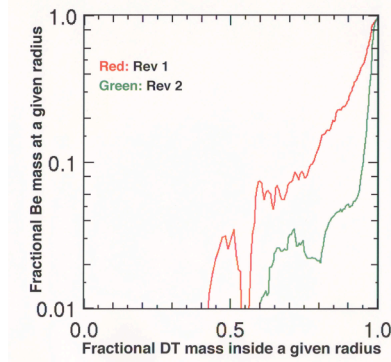


Figure 5. Mass fraction of Be vs. fractional fuel mass for Rev 2 [Green] and Rev 1 [Red], when the core temperature is 8 keV.

Future Work

Although no degradation in neutron yield is seen in these simulations, 1D simulations with a simple mix model indicate that high mode mix does reduce capsule robustness. We plan to examine combinations of high mode mix and other errors, such as low drive or mistimed shocks, to evaluate how the overall margin is affected. We also plan to assess the importance of viscosity and mass diffusion, which will reduce growth at sufficiently high mode numbers, and may be important for our conditions.

* This work was performed under the auspices of U.S. Department of Energy by the Lawrence Livermore National Laboratory under Contract No. W-7405-Eng-48.

¹ S.W. Haan et al, Phys. Plasmas 12, 56316 (2005)

² M.M. Marinak et al, Phys. Plasmas 5, 1125 (1998)

³ During the implosion the scale length varies from $\sim 1 \mu\text{m}$ up to $\sim 3 \mu\text{m}$.

⁴ Y.T. Lee and R.M. More, Plasma Phys. Controlled Fusion 27, 1273 (1984)

⁵ Purgatorio reference

⁶ Rev 1 power spectrum reference

⁷ Spherical interferometer reference

⁸ The capsule acceleration begins after the fourth shock passes through the DT at 12.5 ns. The mix width is defined as the (maximum radius of DT - minimum radius of Be).

⁹ Applied roughness consistent with design specification for this surface

¹⁰ For Rev 2, the Cu concentration in the three inner doped layers is 0.5%, 1.0%, and 0.5% (Reference).